hep-ex/0607055

BABAR-CONF-06/010
SLAC-PUB-11984
July 2006

Measurement of the Branching Fractions of the Decays $\overline{B}^0 \to \Lambda_c^+ \overline{p}$ and $B^- \to \Lambda_c^+ \overline{p} \pi^-$

The *BABAR* Collaboration

July 27, 2006

Abstract

We present studies of two-body and three-body charmed baryonic B decays in a sample of 232 million $B\overline{B}$ pairs collected with the *BABAR* detector at the PEP-II e^+e^- storage ring. The branching fractions of the decays $\bar{B}^0 \to \Lambda_c^+ \bar{p}$ and $B^- \to \Lambda_c^+ \bar{p} \pi^-$ are measured to be $(2.15 \pm 0.36 \pm 0.13 \pm 0.56) \times 10^{-5}$ and $(3.53 \pm 0.18 \pm 0.31 \pm 0.92) \times 10^{-4}$, respectively. The uncertainties quoted are statistical, systematic, and from the $\Lambda_c^+ \to pK^-\pi^+$ branching fraction. We observe a baryon-antibaryon threshold enhancement in the $\Lambda_c^+ \overline{p}$ invariant mass spectrum of the three-body mode and measure the ratio of the branching fractions to be $\mathcal{B}(B^- \to \Lambda_c^+ \overline{p} \pi^-)/\mathcal{B}(\overline{B}^0 \to \Lambda_c^+ \overline{p}) = 16.4 \pm 2.9 \pm 1.4$. These results are preliminary.

Submitted to the 33rd International Conference on High-Energy Physics, ICHEP 06,
26 July—2 August 2006, Moscow, Russia.

Stanford Linear Accelerator Center, Stanford University, Stanford, CA 94309

Work supported in part by the US Department of Energy contract DE-AC02-76SF00515

The *BABAR* Collaboration,

B. Aubert, R. Barate, M. Bona, D. Boutigny, F. Couderc, Y. Karyotakis, J. P. Lees, V. Poireau, V. Tisserand, A. Zghiche

Laboratoire de Physique des Particules, IN2P3/CNRS et Université de Savoie, F-74941 Annecy-Le-Vieux, France

E. Grauges

Universitat de Barcelona, Facultat de Fisica, Departament ECM, E-08028 Barcelona, Spain

A. Palano

Università di Bari, Dipartimento di Fisica and INFN, I-70126 Bari, Italy

J. C. Chen, N. D. Qi, G. Rong, P. Wang, Y. S. Zhu

Institute of High Energy Physics, Beijing 100039, China

G. Eigen, I. Ofte, B. Stugu

University of Bergen, Institute of Physics, N-5007 Bergen, Norway

G. S. Abrams, M. Battaglia, D. N. Brown, J. Button-Shafer, R. N. Cahn, E. Charles, M. S. Gill, Y. Groysman, R. G. Jacobsen, J. A. Kadyk, L. T. Kerth, Yu. G. Kolomensky, G. Kukartsev, G. Lynch, L. M. Mir, T. J. Orimoto, M. Pripstein, N. A. Roe, M. T. Ronan, W. A. Wenzel

Lawrence Berkeley National Laboratory and University of California, Berkeley, California 94720, USA

P. del Amo Sanchez, M. Barrett, K. E. Ford, A. J. Hart, T. J. Harrison, C. M. Hawkes, S. E. Morgan, A. T. Watson

University of Birmingham, Birmingham, B15 2TT, United Kingdom

T. Held, H. Koch, B. Lewandowski, M. Pelizaeus, K. Peters, T. Schroeder, M. Steinke

Ruhr Universität Bochum, Institut für Experimentalphysik 1, D-44780 Bochum, Germany

J. T. Boyd, J. P. Burke, W. N. Cottingham, D. Walker

University of Bristol, Bristol BS8 1TL, United Kingdom

D. J. Asgeirsson, T. Cuhadar-Donszelmann, B. G. Fulsom, C. Hearty, N. S. Knecht, T. S. Mattison, J. A. McKenna

University of British Columbia, Vancouver, British Columbia, Canada V6T 1Z1

A. Khan, P. Kyberd, M. Saleem, D. J. Sherwood, L. Teodorescu

Brunel University, Uxbridge, Middlesex UB8 3PH, United Kingdom

V. E. Blinov, A. D. Bukin, V. P. Druzhinin, V. B. Golubev, A. P. Onuchin, S. I. Serednyakov, Yu. I. Skovpen, E. P. Solodov, K. Yu Todyshev

Budker Institute of Nuclear Physics, Novosibirsk 630090, Russia

D. S. Best, M. Bondioli, M. Bruinsma, M. Chao, S. Curry, I. Eschrich, D. Kirkby, A. J. Lankford, P. Lund, M. Mandelkern, R. K. Mommsen, W. Roethel, D. P. Stoker

University of California at Irvine, Irvine, California 92697, USA

S. Abachi, C. Buchanan

University of California at Los Angeles, Los Angeles, California 90024, USA

S. D. Foulkes, J. W. Gary, O. Long, B. C. Shen, K. Wang, L. Zhang
University of California at Riverside, Riverside, California 92521, USA

H. K. Hadavand, E. J. Hill, H. P. Paar, S. Rahatlou, V. Sharma
University of California at San Diego, La Jolla, California 92093, USA

J. W. Berryhill, C. Campagnari, A. Cunha, B. Dahmes, T. M. Hong, D. Kovalskyi, J. D. Richman
University of California at Santa Barbara, Santa Barbara, California 93106, USA

T. W. Beck, A. M. Eisner, C. J. Flacco, C. A. Heusch, J. Kroseberg, W. S. Lockman, G. Nesom, T. Schalk, B. A. Schumm, A. Seiden, P. Spradlin, D. C. Williams, M. G. Wilson
University of California at Santa Cruz, Institute for Particle Physics, Santa Cruz, California 95064, USA

J. Albert, E. Chen, A. Dvoretskii, F. Fang, D. G. Hitlin, I. Narsky, T. Piatenko, F. C. Porter, A. Ryd, A. Samuel
California Institute of Technology, Pasadena, California 91125, USA

G. Mancinelli, B. T. Meadows, K. Mishra, M. D. Sokoloff
University of Cincinnati, Cincinnati, Ohio 45221, USA

F. Blanc, P. C. Bloom, S. Chen, W. T. Ford, J. F. Hirschauer, A. Kreisel, M. Nagel, U. Nauenberg, A. Olivas, W. O. Ruddick, J. G. Smith, K. A. Ulmer, S. R. Wagner, J. Zhang
University of Colorado, Boulder, Colorado 80309, USA

A. Chen, E. A. Eckhart, A. Soffer, W. H. Toki, R. J. Wilson, F. Winklmeier, Q. Zeng
Colorado State University, Fort Collins, Colorado 80523, USA

D. D. Altenburg, E. Feltresi, A. Hauke, H. Jasper, J. Merkel, A. Petzold, B. Spaan
Universität Dortmund, Institut für Physik, D-44221 Dortmund, Germany

T. Brandt, V. Klose, H. M. Lacker, W. F. Mader, R. Nogowski, J. Schubert, K. R. Schubert, R. Schwierz, J. E. Sundermann, A. Volk
Technische Universität Dresden, Institut für Kern- und Teilchenphysik, D-01062 Dresden, Germany

D. Bernard, G. R. Bonneaud, E. Latour, Ch. Thiebaux, M. Verderi
Laboratoire Leprince-Ringuet, CNRS/IN2P3, Ecole Polytechnique, F-91128 Palaiseau, France

P. J. Clark, W. Gradl, F. Muheim, S. Playfer, A. I. Robertson, Y. Xie
University of Edinburgh, Edinburgh EH9 3JZ, United Kingdom

M. Andreotti, D. Bettoni, C. Bozzi, R. Calabrese, G. Cibinetto, E. Luppi, M. Negrini, A. Petrella, L. Piemontese, E. Prencipe
Università di Ferrara, Dipartimento di Fisica and INFN, I-44100 Ferrara, Italy

F. Anulli, R. Baldini-Ferroli, A. Calcaterra, R. de Sangro, G. Finocchiaro, S. Pacetti, P. Patteri, I. M. Peruzzi,[1] M. Piccolo, M. Rama, A. Zallo
Laboratori Nazionali di Frascati dell'INFN, I-00044 Frascati, Italy

[1]Also with Università di Perugia, Dipartimento di Fisica, Perugia, Italy

A. Buzzo, R. Capra, R. Contri, M. Lo Vetere, M. M. Macri, M. R. Monge, S. Passaggio, C. Patrignani, E. Robutti, A. Santroni, S. Tosi

Università di Genova, Dipartimento di Fisica and INFN, I-16146 Genova, Italy

G. Brandenburg, K. S. Chaisanguanthum, M. Morii, J. Wu

Harvard University, Cambridge, Massachusetts 02138, USA

R. S. Dubitzky, J. Marks, S. Schenk, U. Uwer

Universität Heidelberg, Physikalisches Institut, Philosophenweg 12, D-69120 Heidelberg, Germany

D. J. Bard, W. Bhimji, D. A. Bowerman, P. D. Dauncey, U. Egede, R. L. Flack, J. A. Nash, M. B. Nikolich, W. Panduro Vazquez

Imperial College London, London, SW7 2AZ, United Kingdom

P. K. Behera, X. Chai, M. J. Charles, U. Mallik, N. T. Meyer, V. Ziegler

University of Iowa, Iowa City, Iowa 52242, USA

J. Cochran, H. B. Crawley, L. Dong, V. Eyges, W. T. Meyer, S. Prell, E. I. Rosenberg, A. E. Rubin

Iowa State University, Ames, Iowa 50011-3160, USA

A. V. Gritsan

Johns Hopkins University, Baltimore, Maryland 21218, USA

A. G. Denig, M. Fritsch, G. Schott

Universität Karlsruhe, Institut für Experimentelle Kernphysik, D-76021 Karlsruhe, Germany

N. Arnaud, M. Davier, G. Grosdidier, A. Höcker, F. Le Diberder, V. Lepeltier, A. M. Lutz, A. Oyanguren, S. Pruvot, S. Rodier, P. Roudeau, M. H. Schune, A. Stocchi, W. F. Wang, G. Wormser

Laboratoire de l'Accélérateur Linéaire, IN2P3/CNRS et Université Paris-Sud 11, Centre Scientifique d'Orsay, B.P. 34, F-91898 ORSAY Cedex, France

C. H. Cheng, D. J. Lange, D. M. Wright

Lawrence Livermore National Laboratory, Livermore, California 94550, USA

C. A. Chavez, I. J. Forster, J. R. Fry, E. Gabathuler, R. Gamet, K. A. George, D. E. Hutchcroft, D. J. Payne, K. C. Schofield, C. Touramanis

University of Liverpool, Liverpool L69 7ZE, United Kingdom

A. J. Bevan, F. Di Lodovico, W. Menges, R. Sacco

Queen Mary, University of London, E1 4NS, United Kingdom

G. Cowan, H. U. Flaecher, D. A. Hopkins, P. S. Jackson, T. R. McMahon, S. Ricciardi, F. Salvatore, A. C. Wren

University of London, Royal Holloway and Bedford New College, Egham, Surrey TW20 0EX, United Kingdom

D. N. Brown, C. L. Davis

University of Louisville, Louisville, Kentucky 40292, USA

J. Allison, N. R. Barlow, R. J. Barlow, Y. M. Chia, C. L. Edgar, G. D. Lafferty, M. T. Naisbit, J. C. Williams, J. I. Yi

University of Manchester, Manchester M13 9PL, United Kingdom

C. Chen, W. D. Hulsbergen, A. Jawahery, C. K. Lae, D. A. Roberts, G. Simi

University of Maryland, College Park, Maryland 20742, USA

G. Blaylock, C. Dallapiccola, S. S. Hertzbach, X. Li, T. B. Moore, S. Saremi, H. Staengle

University of Massachusetts, Amherst, Massachusetts 01003, USA

R. Cowan, G. Sciolla, S. J. Sekula, M. Spitznagel, F. Taylor, R. K. Yamamoto

Massachusetts Institute of Technology, Laboratory for Nuclear Science, Cambridge, Massachusetts 02139, USA

H. Kim, S. E. Mclachlin, P. M. Patel, S. H. Robertson

McGill University, Montréal, Québec, Canada H3A 2T8

A. Lazzaro, V. Lombardo, F. Palombo

Università di Milano, Dipartimento di Fisica and INFN, I-20133 Milano, Italy

J. M. Bauer, L. Cremaldi, V. Eschenburg, R. Godang, R. Kroeger, D. A. Sanders, D. J. Summers, H. W. Zhao

University of Mississippi, University, Mississippi 38677, USA

S. Brunet, D. Côté, M. Simard, P. Taras, F. B. Viaud

Université de Montréal, Physique des Particules, Montréal, Québec, Canada H3C 3J7

H. Nicholson

Mount Holyoke College, South Hadley, Massachusetts 01075, USA

N. Cavallo,[2] G. De Nardo, F. Fabozzi,[3] C. Gatto, L. Lista, D. Monorchio, P. Paolucci, D. Piccolo, C. Sciacca

Università di Napoli Federico II, Dipartimento di Scienze Fisiche and INFN, I-80126, Napoli, Italy

M. A. Baak, G. Raven, H. L. Snoek

NIKHEF, National Institute for Nuclear Physics and High Energy Physics, NL-1009 DB Amsterdam, The Netherlands

C. P. Jessop, J. M. LoSecco

University of Notre Dame, Notre Dame, Indiana 46556, USA

T. Allmendinger, G. Benelli, L. A. Corwin, K. K. Gan, K. Honscheid, D. Hufnagel, P. D. Jackson, H. Kagan, R. Kass, A. M. Rahimi, J. J. Regensburger, R. Ter-Antonyan, Q. K. Wong

Ohio State University, Columbus, Ohio 43210, USA

N. L. Blount, J. Brau, R. Frey, O. Igonkina, J. A. Kolb, M. Lu, R. Rahmat, N. B. Sinev, D. Strom, J. Strube, E. Torrence

University of Oregon, Eugene, Oregon 97403, USA

[2]Also with Università della Basilicata, Potenza, Italy
[3]Also with Università della Basilicata, Potenza, Italy

A. Gaz, M. Margoni, M. Morandin, A. Pompili, M. Posocco, M. Rotondo, F. Simonetto, R. Stroili, C. Voci
Università di Padova, Dipartimento di Fisica and INFN, I-35131 Padova, Italy

M. Benayoun, H. Briand, J. Chauveau, P. David, L. Del Buono, Ch. de la Vaissière, O. Hamon, B. L. Hartfiel, M. J. J. John, Ph. Leruste, J. Malclès, J. Ocariz, L. Roos, G. Therin
Laboratoire de Physique Nucléaire et de Hautes Energies, IN2P3/CNRS, Université Pierre et Marie Curie-Paris6, Université Denis Diderot-Paris7, F-75252 Paris, France

L. Gladney, J. Panetta
University of Pennsylvania, Philadelphia, Pennsylvania 19104, USA

M. Biasini, R. Covarelli
Università di Perugia, Dipartimento di Fisica and INFN, I-06100 Perugia, Italy

C. Angelini, G. Batignani, S. Bettarini, F. Bucci, G. Calderini, M. Carpinelli, R. Cenci, F. Forti, M. A. Giorgi, A. Lusiani, G. Marchiori, M. A. Mazur, M. Morganti, N. Neri, E. Paoloni, G. Rizzo, J. J. Walsh
Università di Pisa, Dipartimento di Fisica, Scuola Normale Superiore and INFN, I-56127 Pisa, Italy

M. Haire, D. Judd, D. E. Wagoner
Prairie View A&M University, Prairie View, Texas 77446, USA

J. Biesiada, N. Danielson, P. Elmer, Y. P. Lau, C. Lu, J. Olsen, A. J. S. Smith, A. V. Telnov
Princeton University, Princeton, New Jersey 08544, USA

F. Bellini, G. Cavoto, A. D'Orazio, D. del Re, E. Di Marco, R. Faccini, F. Ferrarotto, F. Ferroni, M. Gaspero, L. Li Gioi, M. A. Mazzoni, S. Morganti, G. Piredda, F. Polci, F. Safai Tehrani, C. Voena
Università di Roma La Sapienza, Dipartimento di Fisica and INFN, I-00185 Roma, Italy

M. Ebert, H. Schröder, R. Waldi
Universität Rostock, D-18051 Rostock, Germany

T. Adye, N. De Groot, B. Franek, E. O. Olaiya, F. F. Wilson
Rutherford Appleton Laboratory, Chilton, Didcot, Oxon, OX11 0QX, United Kingdom

R. Aleksan, S. Emery, A. Gaidot, S. F. Ganzhur, G. Hamel de Monchenault, W. Kozanecki, M. Legendre, G. Vasseur, Ch. Yèche, M. Zito
DSM/Dapnia, CEA/Saclay, F-91191 Gif-sur-Yvette, France

X. R. Chen, H. Liu, W. Park, M. V. Purohit, J. R. Wilson
University of South Carolina, Columbia, South Carolina 29208, USA

M. T. Allen, D. Aston, R. Bartoldus, P. Bechtle, N. Berger, R. Claus, J. P. Coleman, M. R. Convery, M. Cristinziani, J. C. Dingfelder, J. Dorfan, G. P. Dubois-Felsmann, D. Dujmic, W. Dunwoodie, R. C. Field, T. Glanzman, S. J. Gowdy, M. T. Graham, P. Grenier,[4] V. Halyo, C. Hast, T. Hryn'ova, W. R. Innes, M. H. Kelsey, P. Kim, D. W. G. S. Leith, S. Li, S. Luitz, V. Luth, H. L. Lynch, D. B. MacFarlane, H. Marsiske, R. Messner, D. R. Muller, C. P. O'Grady, V. E. Ozcan, A. Perazzo, M. Perl, T. Pulliam, B. N. Ratcliff, A. Roodman, A. A. Salnikov, R. H. Schindler, J. Schwiening, A. Snyder, J. Stelzer, D. Su, M. K. Sullivan, K. Suzuki, S. K. Swain, J. M. Thompson, J. Va'vra, N. van

[4]Also at Laboratoire de Physique Corpusculaire, Clermont-Ferrand, France

Bakel, M. Weaver, A. J. R. Weinstein, W. J. Wisniewski, M. Wittgen, D. H. Wright, A. K. Yarritu, K. Yi, C. C. Young
Stanford Linear Accelerator Center, Stanford, California 94309, USA

P. R. Burchat, A. J. Edwards, S. A. Majewski, B. A. Petersen, C. Roat, L. Wilden
Stanford University, Stanford, California 94305-4060, USA

S. Ahmed, M. S. Alam, R. Bula, J. A. Ernst, V. Jain, B. Pan, M. A. Saeed, F. R. Wappler, S. B. Zain
State University of New York, Albany, New York 12222, USA

W. Bugg, M. Krishnamurthy, S. M. Spanier
University of Tennessee, Knoxville, Tennessee 37996, USA

R. Eckmann, J. L. Ritchie, A. Satpathy, C. J. Schilling, R. F. Schwitters
University of Texas at Austin, Austin, Texas 78712, USA

J. M. Izen, X. C. Lou, S. Ye
University of Texas at Dallas, Richardson, Texas 75083, USA

F. Bianchi, F. Gallo, D. Gamba
Università di Torino, Dipartimento di Fisica Sperimentale and INFN, I-10125 Torino, Italy

M. Bomben, L. Bosisio, C. Cartaro, F. Cossutti, G. Della Ricca, S. Dittongo, L. Lanceri, L. Vitale
Università di Trieste, Dipartimento di Fisica and INFN, I-34127 Trieste, Italy

V. Azzolini, N. Lopez-March, F. Martinez-Vidal
IFIC, Universitat de Valencia-CSIC, E-46071 Valencia, Spain

Sw. Banerjee, B. Bhuyan, C. M. Brown, D. Fortin, K. Hamano, R. Kowalewski, I. M. Nugent, J. M. Roney, R. J. Sobie
University of Victoria, Victoria, British Columbia, Canada V8W 3P6

J. J. Back, P. F. Harrison, T. E. Latham, G. B. Mohanty, M. Pappagallo
Department of Physics, University of Warwick, Coventry CV4 7AL, United Kingdom

H. R. Band, X. Chen, B. Cheng, S. Dasu, M. Datta, K. T. Flood, J. J. Hollar, P. E. Kutter, B. Mellado, A. Mihalyi, Y. Pan, M. Pierini, R. Prepost, S. L. Wu, Z. Yu
University of Wisconsin, Madison, Wisconsin 53706, USA

H. Neal
Yale University, New Haven, Connecticut 06511, USA

1 INTRODUCTION

Charmed baryonic B decays are experimentally accessible and provide a way to check predictions given by various theoretical models for exclusive baryonic B decays. There is theoretical interest in the suppression of the two-body baryonic decay rates compared to three-body decay rates and the possible connection to production mechanisms for baryons in B decays. Analysis of the charmed three-body baryonic B decay reveals that the invariant mass of the baryon-antibaryon system is peaked near threshold [1]. Charmless two-body baryonic B decays (which have not yet been observed [2, 3]) may be used to measure direct CP violation in the B system. Their charmed counterparts, however, have branching fractions at least an order of magnitude higher than the charmless modes, and thus can help distinguish between theoretical models that predict the charmless decay rates of B mesons to baryons. The Feynman diagrams for these decays are shown in Figure 1, in which the B meson decays weakly via internal W emission to $\Lambda_c^+\overline{p}(\pi)$.

Charmed baryonic B decays have recently been measured by the CLEO [4] and Belle [1, 5, 6] Collaborations. In particular, the Belle Collaboration has measured the branching fractions of the modes[5] $\overline{B}^0 \to \Lambda_c^+\overline{p}$ (using 85 million $B\overline{B}$ pairs) [5] and $B^- \to \Lambda_c^+\overline{p}\pi^-$ (using 152 million $B\overline{B}$ pairs) [1]:

$$\mathcal{B}(\overline{B}^0 \to \Lambda_c^+\overline{p}) = (2.19^{+0.56}_{-0.49} \pm 0.32 \pm 0.57) \times 10^{-5} \text{ and}$$
$$\mathcal{B}(B^- \to \Lambda_c^+\overline{p}\pi^-) = (20.1 \pm 1.5 \pm 2.0 \pm 5.2) \times 10^{-5},$$

where the errors are statistical, systematic, and from the $\Lambda_c^+ \to pK^-\pi^+$ branching fraction, respectively. *BABAR* has collected nearly three times the data used in the Belle analysis of the two-body mode, and we can therefore perform a more precise measurement of this branching fraction. For now, the measurement errors are dominated by the 26% fractional error on $\mathcal{B}(\Lambda_c^+ \to pK^-\pi^+) = (5.0 \pm 1.3)\%$ [7], but this uncertainty cancels in the ratio of the three-body to two-body branching fractions.

The excess of events near the baryon-antibaryon production threshold seen by Belle in $B^- \to \Lambda_c^+\overline{p}\pi^-$ has also been observed in $B^0 \to \overline{\Lambda}p\pi^-$ [8] and several $B \to p\overline{p}X$ [9, 10] modes. In refer-

[5]Throughout this paper, whenever a mode is given, the charge conjugate is also implied.

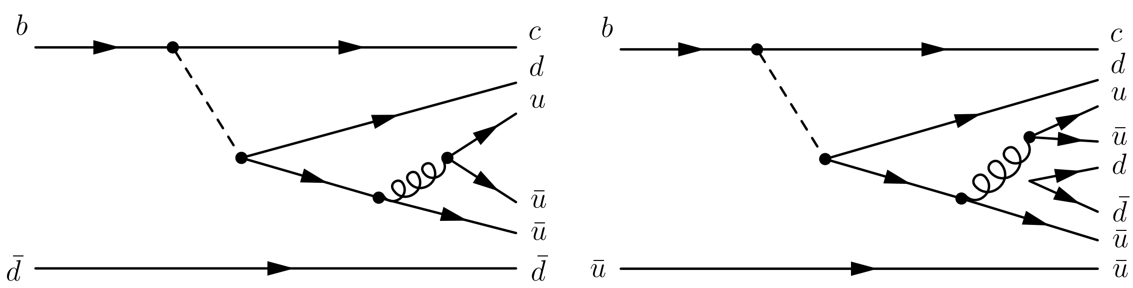

(a) (b)

Figure 1: Feynman diagrams for (a) $\overline{B}^0 \to \Lambda_c^+\overline{p}$ and (b) $B^- \to \Lambda_c^+\overline{p}\pi^-$, in which the B meson decays weakly via internal W emission.

ence [11] a qualitative explanation of the larger three-body branching fraction in conjunction with this threshold effect is given. In the two-body decay, the invariant mass of the baryon-antibaryon is simply m_B, whereas in the three-body decay, the invariant mass of the baryon-antibaryon can be lower, allowing the baryon-antibaryon to form a quasi-resonance near threshold. The third daughter, the meson, carries away much of the energy. The result, regardless of the interpretation of the threshold enhancement, is that the B favors three-body baryonic decay modes by an order of magnitude over two-body modes.

In this analysis, we measure the branching fractions for $\overline{B}^0 \to \Lambda_c^+ \overline{p}$ and $B^- \to \Lambda_c^+ \overline{p} \pi^-$ and observe the threshold enhancement in the baryon-antibaryon system of the the $B^- \to \Lambda_c^+ \overline{p} \pi^-$ mode.

2 THE *BABAR* DETECTOR AND DATASET

The data used in this analysis were collected with the *BABAR* detector at the PEP-II e^+e^- storage ring. The data sample used comprises an integrated luminosity of $210\,\mathrm{fb}^{-1}$ (232 million $B\overline{B}$ pairs) collected from e^+e^- collisions at the $\Upsilon(4S)$ resonance. The *BABAR* detector is described elsewhere [12]. Exclusive B meson decays are simulated with the Monte Carlo (MC) event generator `EvtGen` [13] and hadronization (e.g. for continuum $q\overline{q}$ events) is simulated with `Jetset7.4` [14]. The detector is modeled using the `GEANT4` simulation package [15].

3 ANALYSIS METHOD

3.1 Candidate Selection

We reconstruct Λ_c^+ candidates in the decay mode $\Lambda_c^+ \to pK^-\pi^+$, applying a geometric constraint on the $pK^-\pi^+$ vertex, which is required to have a χ^2 probability greater then 0.1%. The $pK^-\pi^+$ invariant mass must be between 2.275 and $2.295\,\mathrm{GeV}/c^2$. The $pK^-\pi^+$ candidates are constrained to the mass of the Λ_c^+ [7], which provides better resolution in the kinematic variable $\Delta E = E_B^* - \sqrt{s}/2$, where E_B^* is the B candidate energy in the e^+e^- center-of-mass (CM) frame and $\sqrt{s}$ is the total CM energy. Λ_c^+ candidates are then combined in a geometric fit with a $\overline{p}$ (and π) to form a $\overline{B}^0$ (B^-) candidate for the $\overline{B}^0 \to \Lambda_c^+ \overline{p}$ ($B^- \to \Lambda_c^+ \overline{p} \pi^-$) mode. The χ^2 probability for the fit to the full decay tree must be greater than 0.1%.

Daughter p, K, and π candidates must be well-reconstructed in the drift chamber and are identified with likelihood-based particle selectors using information from the silicon vertex tracker, drift chamber, and ring-imaging Čerenkov detector. Several requirements differ between the two- and three-body modes. The pions in the $B^- \to \Lambda_c^+ \overline{p} \pi^-$ mode have lower momenta; therefore, we apply looser drift chamber tracking requirements to improve the efficiency in several areas of the $\Lambda_c^+ \overline{p} \pi^-$ Dalitz plane. The daughter particles in both decay modes have very loose particle identification requirements with two exceptions: 1) the pions in $B^- \to \Lambda_c^+ \overline{p} \pi^-$ are required to satisfy stronger kaon and electron rejection criteria, and 2) the B daughter p in $\overline{B}^0 \to \Lambda_c^+ \overline{p}$ must pass a tight constraint on the likelihood that the track is a proton and stronger electron rejection.

We construct a linear (Fisher) discriminant $\mathcal{F}$ from several event-shape variables to provide continuum suppression: $|\cos\theta^*|$ (θ^* is the angle of the B candidate momentum vector with respect to the beam axis in the e^+e^- CM frame), $|\cos\theta^B_{thr}|$ (θ^B_{thr} is the angle of the B candidate thrust axis with respect to the beam axis in the e^+e^- CM frame), and the summed momentum of the rest of the charged and neutral particles in the event in nine cones centered around the thrust axis of the B candidate. The requirement on $\mathcal{F}$ provides powerful background rejection (72.8%) for the two-body mode, but is less effective for the three-body mode (28.0%) due to a larger component of combinatoric B backgrounds compared to the continuum component. These values were determined by maximizing $N_s/\sqrt{N_s + N_b}$, where N_s is the number of signal events based on signal MC samples and N_b is the number of background events in ΔE upper sidebands ($\Delta E > 0.1\,\mathrm{GeV}$ and $5.2 < m_{\mathrm{ES}} < 5.29\,\mathrm{GeV}/c^2$) in data.

We identify signal candidates using ΔE and the beam-energy-substituted mass $m_{\mathrm{ES}} = \sqrt{((s/2 + \mathbf{p}_i \cdot \mathbf{p}_B)^2/E_i^2 - \mathbf{p}_B^2)}$, where $(E_i, \mathbf{p}_i)$ is the four-momentum of the initial e^+e^- system and $\mathbf{p}_B$ is the momentum of the B candidate, both measured in the laboratory frame. The distribution of ΔE vs. m_{ES} for both modes is shown in Figure 2. We define the fit region to be $-0.1 < \Delta E < 0.1\,\mathrm{GeV}$ and $5.20 < m_{\mathrm{ES}} < 5.29\,\mathrm{GeV}/c^2$ (also indicated in Figure 2). This excludes the ΔE sideband used in the optimization and the region below $-0.1\,\mathrm{GeV}$ in ΔE, which contains backgrounds that peak in m_{ES} but are shifted in ΔE. These backgrounds are from $B \to \Lambda_c p\pi\pi$ ($B \to \Lambda_c p\pi$) events where a B daughter π is not included in the B candidate, mimicking the mode of interest: $B^- \to \Lambda_c^+ \overline{p}\pi^-$ ($\overline{B}^0 \to \Lambda_c^+ \overline{p}$). Studies of exclusive MC samples of these backgrounds indicate that much of the contribution is from $B \to \Sigma_c p\pi$ ($B \to \Sigma_c p$) where a π^0 or slow charged π from the $\Sigma_c \to \Lambda_c\pi$ decay is missed. MC samples comprised of continuum $q\overline{q}$ events and B meson decays were studied to rule out any background that peaks in both ΔE and m_{ES}.

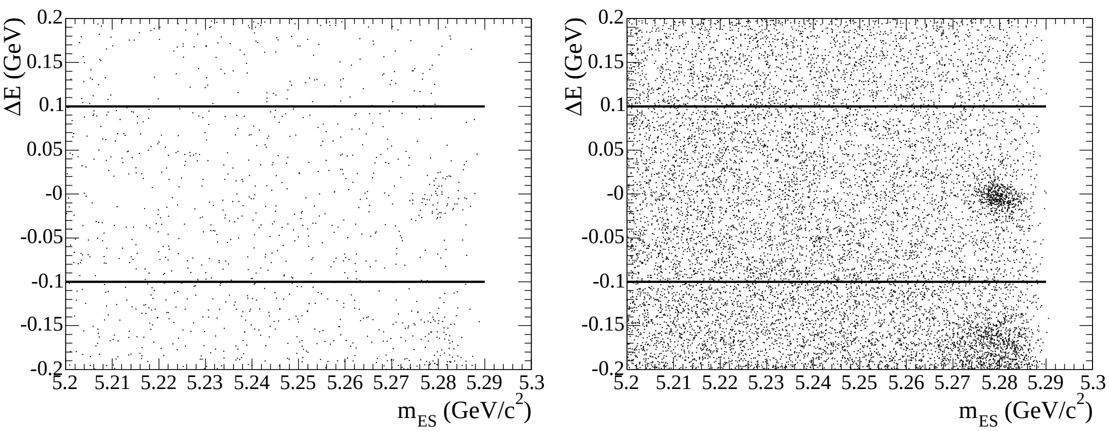

(a) $\overline{B}^0$ candidates in data for $\overline{B}^0 \to \Lambda_c^+ \overline{p}$ (b) B^- candidates in data for $B^- \to \Lambda_c^+ \overline{p}\pi^-$

Figure 2: Distribution of ΔE vs. m_{ES} of B candidates in data for both the two-body (a) and three-body (b) decay modes. The fit regions are indicated.

3.2 $\overline{B}^0 \to \Lambda_c^+ \overline{p}$ Maximum Likelihood Fit

In the analysis of the two-body $\overline{B}^0 \to \Lambda_c^+ \overline{p}$ mode, we did not look at the signal region until the event selection criteria and fit procedures were determined. The efficiency for reconstructing and selecting $\overline{B}^0 \to \Lambda_c^+ \overline{p}$ candidates is 20.2%, and is determined from a fit to the $\overline{B}^0 \to \Lambda_c^+ \overline{p}$ signal MC sample. A 2-D unbinned maximum likelihood fit is performed in ΔE and m_{ES} to extract the

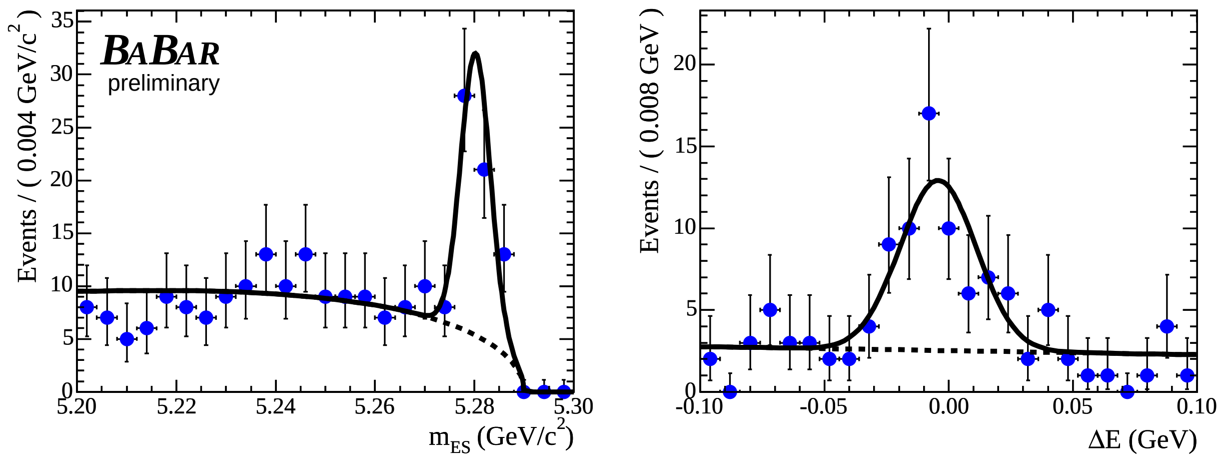

Figure 3: Projections of the 2-D fit in ΔE and $m_{\rm ES}$ for $\Lambda_c^+\overline{p}$ candidates satisfying $|\Delta E| < 0.04\,\mathrm{GeV}$ (left) and $m_{\rm ES} > 5.27\,\mathrm{GeV}/c^2$ (right). The signal yield is 50 ± 8 events, with a significance of 9.4σ.

number of signal events. The background is described by the product of a linear function in ΔE and a threshold function [16] in $m_{\rm ES}$; the signal is described by a single Gaussian distribution in each dimension. All parameters except the $m_{\rm ES}$ threshold are unconstrained in the fit to data. We validate the fitting procedure on a combined sample of signal MC events (over a range of the expected number of signal events) and "toy" MC events (generated according to the shape of the continuum and $B\overline{B}$ MC background events) to ensure that the fit is robust and unbiased.

The results of the fit to data are shown in Figure 3; we obtain 50 ± 8 signal events and a significance of $\sqrt{-2\ln(\mathcal{L}_0/\mathcal{L}_{max})} = 9.4\sigma$, where $\mathcal{L}_{max}$ is the maximum likelihood from the fit result and $\mathcal{L}_0$ is the maximum likelihood when the signal yield is fixed to zero. The mean in ΔE is shifted slightly below zero ($-4.2 \pm 2.7\,\mathrm{MeV}$); this shift is in the appropriate direction given that the Λ_c^+ mass is constrained to the 2004 PDG value [7] which is approximately $1.5\,\mathrm{MeV}$ lower than the most recent measurement [17]. The ΔE resolution, $15.4 \pm 2.1\,\mathrm{MeV}$, is slightly larger than, but consistent with, the resolution in MC ($13.6 \pm 0.1\,\mathrm{MeV}$).

3.3 $B^- \rightarrow \Lambda_c^+\overline{p}\pi^-$ Maximum Likelihood Fit

For the three-body $B^- \rightarrow \Lambda_c^+\overline{p}\pi^-$ mode, a 2-D unbinned maximum likelihood fit is also performed. Again, all parameters except the $m_{\rm ES}$ threshold are unconstrained in the fit to data. The background PDF is the same as in the two-body mode, but the signal PDF consists of a Gaussian in ΔE times a Gaussian in $m_{\rm ES}$, where a correlation is allowed between the two observables. This was not necessary in the two-body mode due to the limited number of signal events. The signal PDF also contains an additional uncorrelated Gaussian component in ΔE with the same mean as the correlated Gaussian but an independent width. This signal PDF was chosen from a study of $B^- \rightarrow \Lambda_c^+\overline{p}\pi^-$ signal MC events along with extensive studies of various PDFs using a combined sample of signal MC and toy MC events. These studies showed this PDF to have the smallest bias: -8 ± 2 events for 500 total signal events (the level of bias is consistent for a range of signal events). The result of the fit to data with this PDF is shown in Figure 4. The signal yield from the fit is 571 ± 34 events and the ΔE resolution (RMS) is $19 \pm 3\,\mathrm{MeV}$.

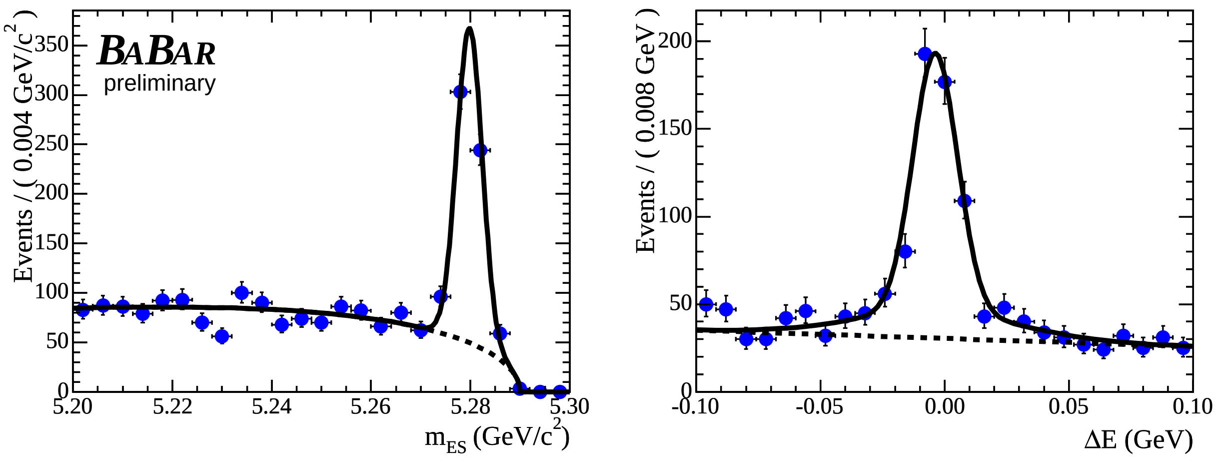

Figure 4: Projections of the 2-D fit in m_{ES} and ΔE, for $\Lambda_c^+ \overline{p}\pi^-$ candidates satisfying $|\Delta E| < 0.030\,\mathrm{GeV}$ (left) and $m_{\mathrm{ES}} > 5.27\,\mathrm{GeV}/c^2$ (right). This 2-D fit is used to extract the likelihood that each event is a signal or background event. The signal yield is 571 ± 34 events.

3.4 $B^- \to \Lambda_c^+ \overline{p}\pi^-$ Yield Extraction and Efficiency Correction

We use the ${}_s\mathcal{P}lot$ technique [18] (a sophisticated background subtraction method) to project out the signal and background distributions separately based on the 2-D fit to ΔE and m_{ES}. We calculate a signal weight for each event i according to the following equation:

$$W_i = \frac{f_s(m_{\mathrm{ES}i}, \Delta E_i) + \mathrm{V}_{sb} f_b(m_{\mathrm{ES}i}, \Delta E_i)}{N_s f_s(m_{\mathrm{ES}i}, \Delta E_i) + N_b f_b(m_{\mathrm{ES}i}, \Delta E_i)}, \tag{1}$$

where W_i is the ${}_s\mathcal{P}lot$ weight, $N_s(N_b)$ is the number of fitted signal (background) events, and $f_s(f_b)$ is the signal (background) PDF. V_{sb} is the off-diagonal element of a 2×2 covariance matrix calculated directly from data, with all parameters fixed to their fitted values except for the signal and background yields. A background weight for each event can be calculated in an analogous manner. The result of this method is that each event is assigned a signal and background weight, which can be plotted for any quantity that is uncorrelated with ΔE and m_{ES}. The quantities of interest that satisfy this requirement are the invariant masses $m_{d_i d_j}$, where d_i is any of the B daughters Λ_c^+, $\overline{p}$, π^-. The correlations of ΔE and m_{ES} with these quantities are less than 5%. The ${}_s\mathcal{P}lot$ method relies on using the events in the entire fit region to provide good sampling of both signal and background. However, (background) events that have an invariant $\Lambda_c^+ \overline{p}\pi^-$ mass far from the mass of the B meson have a different kinematically allowed Dalitz region than (signal) events with an invariant $\Lambda_c^+ \overline{p}\pi^-$ mass close to m_B. We calculate $m_{d_i d_j}$ with a B mass constraint so that all of the B candidates in the fit region lie in the same Dalitz region.

The detection efficiency for $B^- \to \Lambda_c^+ \overline{p}\pi^-$ events varies significantly across the Dalitz plane. Therefore, using the average nonresonant MC efficiency (15.3%) to calculate the branching fraction for this mode is insufficient. Instead, an efficiency correction is applied to each signal event based on its location in the Dalitz plane. We divide the physical region into 215 equal-size bins and determine the efficiency in each bin; a plot of this efficiency for $m^2_{p\pi}$ vs. $m^2_{\Lambda_c\pi}$ is shown in Figure 5.

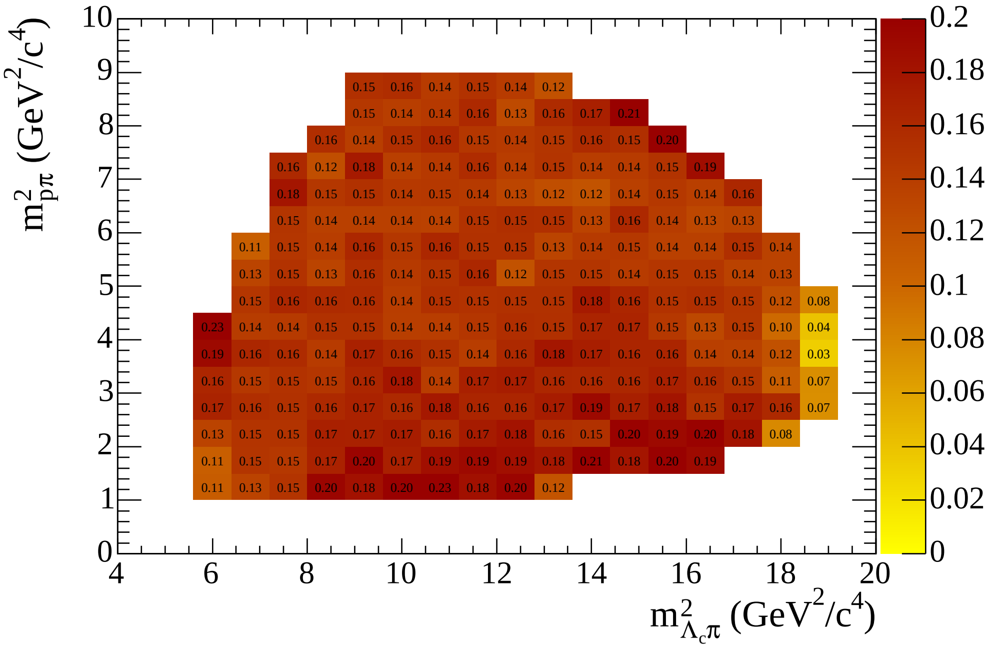

Figure 5: Binned efficiency for $m^2_{p\pi}$ vs. $m^2_{\Lambda_c\pi}$ in the kinematically allowed region of the Dalitz plane.

There are noticeable deficiencies in the lower left (right) corners of the $\Lambda_c^+\overline{p}\pi^-$ Dalitz plane, where the π (Λ_c) candidates have low momentum in the B rest frame. The looser tracking requirements on the pions help to compensate for this effect, but do not eliminate it entirely. We build on the ${}_s\mathcal{P}lot$ formalism to individually correct each event by an additional weight, $1/\varepsilon_{\alpha\beta}$, where $\varepsilon_{\alpha\beta}$ is the efficiency in bin (α,β). We define an "effective" efficiency ($\varepsilon_{\rm eff}$) as the signal yield from the fit divided by the number of ${}_s\mathcal{P}lot$-weighted, efficiency-corrected events. The effective efficiency for selecting B candidates in the three-body mode is $\varepsilon_{\rm eff} = 14.2\%$.

4 SYSTEMATIC STUDIES

Various sources of systematic uncertainties have been investigated, including those related to the total number of $B\overline{B}$ pairs in data, the method used to determine the efficiency from MC, and the fitting procedures. These are summarized for both modes in Table 1. Note that for the branching fraction measurement of $\overline{B}^0 \rightarrow \Lambda_c^+\overline{p}$, the statistical error dominates over the total systematic uncertainty.

The systematic uncertainty on the number of $B\overline{B}$ pairs produced by *BABAR* is 1.1%.

There are several sources of systematic uncertainty related to the efficiency determinations. The statistical uncertainty due to the number of signal MC events contributes a 1.0% systematic error on the efficiency. Tracking efficiency systematic errors are based on studies of τ decays, which yield an uncertainty of 0.8% per track. However, this is reduced to 0.6% for the higher momentum B daughter p in the two-body mode and increased to 1.4% for the lower momentum pions in the three-body mode. Particle identification is determined using large control samples,

Table 1: Summary of the contributions to the total systematic uncertainty. The total is determined by adding the uncertainty from each source in quadrature.

Source	Systematic Uncertainty	
	$\overline{B}^0 \to \Lambda_c^+ \overline{p}$	$B^- \to \Lambda_c^+ \overline{p} \pi^-$
$N_{B\overline{B}}$	1.1%	1.1%
MC statistics	1.0%	4.7%
Dalitz binning	–	2.0%
Tracking	3.0%	5.2%
PID	4.7%	1.2%
Fitting	2.2%	4.5%
Total	6.0%	8.7%

which may differ from the modes we are investigating due to the higher multiplicities of these charmed baryonic B decays and other subtleties. Differences between the momentum spectra and angular distributions of the daughter particles compared to those in the control samples are used to assess a systematic uncertainty on the efficiency due to particle identification. In $\overline{B}^0 \to \Lambda_c^+ \overline{p}$, we assign a 2.5% systematic uncertainty to the B daughter $\overline{p}$, and a (1.5 to 1.7)% uncertainty on the other daughter particles. In $B^- \to \Lambda_c^+ \overline{p} \pi^-$, the systematic uncertainty due to particle identification varies from (0.1 to 0.9)% per track; the total is 1.2%.

The fitting systematics are studied by varying the background shape in ΔE and the endpoint of the threshold function in $m_{\rm ES}$. This yields a systematic uncertainty of 2.2% for the two-body mode and 0.9% for the three-body mode. The branching fraction measurement of $B^- \to \Lambda_c^+ \overline{p} \pi^-$ has additional systematic uncertainties due to the signal PDF. We assign 4.3% due to the fit bias, the source of which is mostly in the the tails of ΔE. This systematic uncertainty compensates for the inability of the MC to accurately simulate the behavior of the events in these tails. For the three-body mode, we perform the fit to data with and without a correlation between ΔE and $m_{\rm ES}$ in the signal PDF, yielding a systematic uncertainty of 1.1%.

5 RESULTS

The branching fraction of $\overline{B}^0 \to \Lambda_c^+ \overline{p}$ [19], measured with the sample of 232 million $B\overline{B}$ pairs, is

$$\mathcal{B}(\overline{B}^0 \to \Lambda_c^+ \overline{p}) = (2.15 \pm 0.36 \pm 0.13 \pm 0.56) \times 10^{-5},$$

where the errors are statistical, systematic, and from the $\Lambda_c^+ \to pK^-\pi^+$ branching fraction, respectively. The significance of the signal is 9.4σ. This measurement is consistent with a previous Belle measurement of $(2.19^{+0.56}_{-0.49} \pm 0.32 \pm 0.57) \times 10^{-5}$ made with 85 million $B\overline{B}$ pairs. The systematic uncertainty is much lower (6% compared to 15%) than that for the Belle measurement. We also find this measurement to be consistent with the predicted limit from reference [20]: $\mathcal{B}(\overline{B}^0 \to \Lambda_c^+ \overline{p}) \lesssim 7.9 \times 10^{-6}\,|g/5|^2$, where $|g| = 6$–10.

We calculate the total branching fraction of $B^- \to \Lambda_c^+ \overline{p} \pi^-$ as follows:

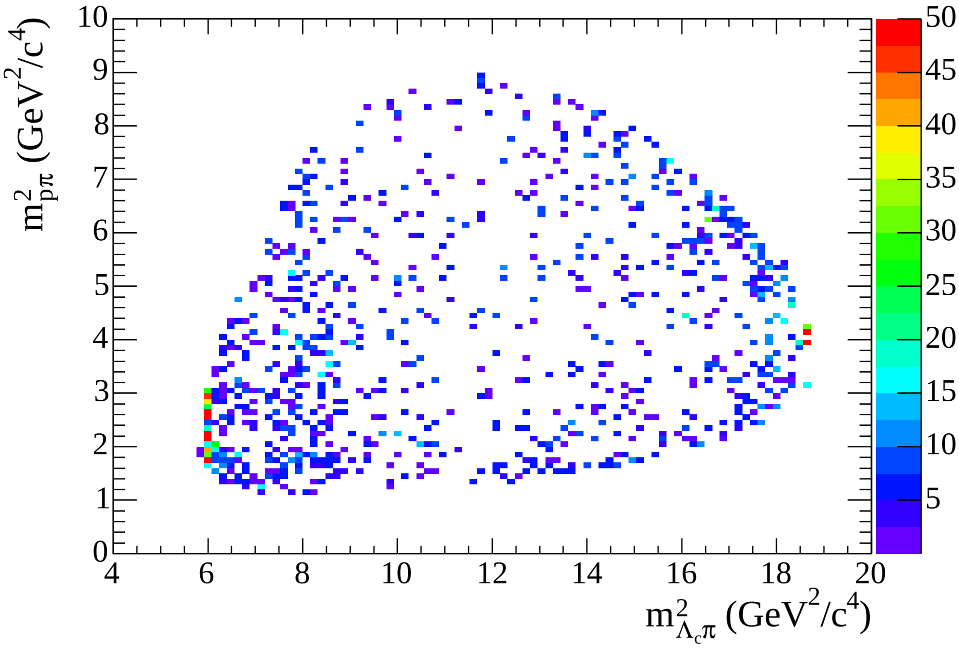

Figure 6: $m^2_{p\pi}$ vs. $m^2_{\Lambda_c\pi}$ for signal B candidates with ${}_s\mathcal{P}lot$ and efficiency correction weights applied. Bins with negative population are suppressed.

$$\begin{aligned}\mathcal{B}(B^- \to \Lambda_c^+ \overline{p} \pi^-)_{tot} &= \frac{(1+b)\sum_i \frac{W_i}{\varepsilon_i}}{N_{B\overline{B}} \times \mathcal{B}(\Lambda_c^+ \to pK^-\pi^+)} \\ &= (3.53 \pm 0.18 \pm 0.31 \pm 0.92) \times 10^{-4},\end{aligned} \tag{2}$$

where the fit bias b is 1.6%, W_i is the signal ${}_s\mathcal{P}lot$ weight and ε_i is the efficiency for event i, and $N_{B\overline{B}}$ is the number of $B\overline{B}$ pairs. The uncertainties are statistical, systematic, and the error on the $\Lambda_c^+ \to pK^-\pi^+$ branching fraction, respectively. This measurement is $3.5\,\sigma$ higher (assuming Gaussian statistics) than the Belle measurement of $\mathcal{B}(B^- \to \Lambda_c^+ \overline{p}\pi^-)_{tot} = (2.01 \pm 0.15 \pm 0.20 \pm 0.52) \times 10^{-4}$. An examination of the Dalitz plot shows a systematic trend in that we measure consistently larger branching fractions in all regions.

The $\Lambda_c^+ \overline{p}\pi^-$ Dalitz plane in data is shown in Figure 6 with ${}_s\mathcal{P}lot$ weights and efficiency corrections applied to each B candidate. We project this onto the $m_{\Lambda_c p}$ axis with the requirement $m_{\Lambda_c\pi} > 2.6\,\mathrm{GeV}/c^2$ (to remove the contribution from the $\Sigma_c(2455)^0$) in Figure 7. We observe a baryon-antibaryon threshold enhancement in the $\Lambda_c^+\overline{p}$ invariant mass spectrum, confirming the large body of evidence supporting the existence of these threshold enhancements in three-body baryonic B decays.

We also report the ratio of the branching fractions of $B^- \to \Lambda_c^+\overline{p}\pi^-$ to $\overline{B}^0 \to \Lambda_c^+\overline{p}$:

$$\frac{\mathcal{B}(B^- \to \Lambda_c^+ \overline{p}\pi^-)}{\mathcal{B}(\overline{B}^0 \to \Lambda_c^+ \overline{p})} = 16.4 \pm 2.9 \pm 1.4. \tag{3}$$

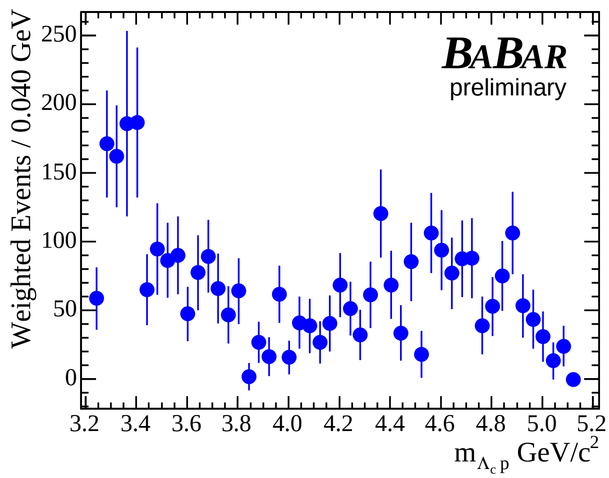

Figure 7: Dalitz plot projection onto the $m_{\Lambda_c p}$ axis with the requirement $m_{\Lambda_c \pi} > 2.6\,\mathrm{GeV}/c^2$, removing the contribution from the $\Sigma_c(2455)^0$. ${}_s\mathcal{P}lot$ weighted, efficiency-corrected signal events are shown. The baryon-antibaryon threshold enhancement is visible near $3.3\,\mathrm{GeV}/c^2$.

Table 2: Comparison of the yields, efficiencies (effective for the three-body decay), and branching fractions for $\overline{B}^0 \to \Lambda_c^+ \overline{p}$ and $B^- \to \Lambda_c^+ \overline{p} \pi^-$.

Mode	Signal yield	$\varepsilon_{(\mathrm{eff})}$	$\mathcal{B}$
$\overline{B}^0 \to \Lambda_c^+ \overline{p}$	50 ± 8	20.2%	$(2.15 \pm 0.36 \pm 0.13 \pm 0.56) \times 10^{-5}$
$B^- \to \Lambda_c^+ \overline{p} \pi^-$	571 ± 34	14.2%	$(3.53 \pm 0.18 \pm 0.31 \pm 0.92) \times 10^{-4}$

The systematic uncertainties on the number of $B\overline{B}$ pairs, the Λ_c^+ daughter p and K tracking, and the Λ_c^+ daughter K and B daughter p particle identification all cancel, as does the uncertainty on $\mathcal{B}(\Lambda_c^+ \to p K^- \pi^+)$. This ratio is consistent with theoretical predictions.

6 SUMMARY

We report the branching fractions of two charmed baryonic B decay modes. Table 2 compares the yields, efficiencies, and branching fractions of the two modes. The total three-body branching fraction measured is significantly larger than that measured by Belle, but is still consistent with (and perhaps provides stronger evidence for) the observation that the three-body mode is enhanced over the two-body mode. The measurement of the ratio of three-body to two-body branching fractions and the observation of the baryon-antibaryon threshold enhancement aid in theoretical interpretations of baryon production in B decays.

7 ACKNOWLEDGMENTS

We are grateful for the extraordinary contributions of our PEP-II colleagues in achieving the excellent luminosity and machine conditions that have made this work possible. The success of this project also relies critically on the expertise and dedication of the computing organizations that support *BABAR*. The collaborating institutions wish to thank SLAC for its support and the kind hospitality extended to them. This work is supported by the US Department of Energy and National Science Foundation, the Natural Sciences and Engineering Research Council (Canada), Institute of High Energy Physics (China), the Commissariat à l'Energie Atomique and Institut National de Physique Nucléaire et de Physique des Particules (France), the Bundesministerium für Bildung und Forschung and Deutsche Forschungsgemeinschaft (Germany), the Istituto Nazionale di Fisica Nucleare (Italy), the Foundation for Fundamental Research on Matter (The Netherlands), the Research Council of Norway, the Ministry of Science and Technology of the Russian Federation, Ministerio de Educación y Ciencia (Spain), and the Particle Physics and Astronomy Research Council (United Kingdom). Individuals have received support from the Marie-Curie IEF program (European Union) and the A. P. Sloan Foundation.

References

[1] Belle Collaboration, K. Abe *et al.*, hep-ex/0409005, presented at ICHEP 2004.

[2] *BABAR* Collaboration, B. Aubert *et al.*, Phys. Rev. D **69**, 091503 (2004).

[3] Belle Collaboration, K. Abe *et al.*, Phys. Rev. D **71**, 072007 (2005).

[4] CLEO Collaboration, S. A. Dytman *et al.*, Phys. Rev. D **66**, 091101 (2002).

[5] Belle Collaboration, N. Gabyshev *et al.*, Phys. Rev. Lett. **90**, 12 (2003).

[6] Belle Collaboration, N. Gabyshev *et al.*, Phys. Rev. D **66**, 091102 (2002).

[7] Particle Data Group, S. Eidelman *et al.*, Phys. Lett. B **152**, 1 (2004).

[8] Belle Collaboration, M.-Z. Wang *et al.*, Phys. Rev. Lett. **90**, 201802 (2003).

[9] Belle Collaboration, M.-Z. Wang *et al.*, Phys. Rev. Lett. **92**, 131901 (2004).

[10] *BABAR* Collaboration, B. Aubert *et al.*, Phys. Rev. D **72**, 051101 (2005).

[11] H. Y. Cheng, J. Korean Phys. Soc. **45**, S245 (2004).

[12] *BABAR* Collaboration, B. Aubert *et al.*, Nucl. Instrum. Methods Phys. Res., Sect. A **479**, 1 (2002).

[13] D. J. Lange, Nucl. Instrum. Methods Phys. Res., Sect. A **462**, 152 (2001).

[14] T. Sjostrand *et al.*, JHEP 0605, 026 (2006).

[15] S. Agostinelli *et al.* (GEANT4 Collaboration), Nucl. Instrum. Methods Phys. Res., Sect. A **506**, 250 (2003).

[16] ARGUS Collaboration, H. Albrecht *et al.*, Z. Phys. C **48**, 543 (1990).

[17] *BABAR* Collaboration, B. Aubert *et al.*, Phys. Rev. D **72**, 052006 (2005).

[18] M. Pivk and F. R. Le Diberder, Nucl. Instr. Methods Phys. Res., Sect. A **555**, 356 (2005).

[19] J. Kroseberg, presented at 41st Rencontres de Moriond: QCD and Hadronic Interactions, La Thuile, Italy, 18-25 Mar 2006, hep-ex/0607011.

[20] H. Y. Cheng and K. C. Yang, Phys. Rev. D **67**, 034008 (2003).